ELSEVIER

Chemical Physics 267 (2001) 277–289

Chemical Physics

www.elsevier.nl/locate/chemphys

# Attosecond time-scale feedback control of coherent X-ray generation

Randy Bartels *, Sterling Backus, Ivan Christov [1], Henry Kapteyn, Margaret Murnane

*JILA, University of Colorado, Campus Box 440, Boulder, CO 80309-0440, USA*

Received 29 September 2000

**Abstract**

High-harmonic generation is an extreme, high-order, nonlinear process that converts intense, ultrafast, visible and infrared laser light pulses coherently into the soft X-ray region of the spectrum. We demonstrate that by optimizing the shape of an ultrafast laser pulse, we can selectively enhance this process by promoting strong constructive interference between X-ray bursts emitted from adjacent optical cycles. This work demonstrates that coherent control of highly nonlinear processes in the strong-field regime is possible by adjusting the relative timing of the crests of an electromagnetic wave on a sub-optical cycle, attosecond time scale. © 2001 Elsevier Science B.V. All rights reserved.

## 1. Introduction

The development of high-power femtosecond lasers [1,2] with pulse durations of a few optical cycles has led to the emergence of a new research area of ''extreme'' nonlinear optics [3–6]. The process of high-harmonic generation (HHG) is a beautiful example of such a process, that can be understood from both a quantum and semi-classical point of view [7,8]. In HHG, an intense femtosecond laser is focused into a gas. The interaction of the intense laser light with the atoms in the gas is so highly nonlinear that high harmonics of the laser frequency are radiated in the forward direction. These harmonics extend from the ultraviolet (UV) to the soft X-ray (XUV) region of the spectrum, up to orders greater than 300. Because all of the atoms in the laser interaction region experience a similar, coherent light field, the X-ray emissions from individual atoms are mutually coherent.

HHG is a very interesting candidate for coherent or feedback control experiments for a number of reasons. First, the HHG X-ray emission has a well-defined phase relationship to the oscillations of the laser field [9,10], as explained below. Second, HHG is one of the highest-order coherent nonlinear-optical interactions yet observed. Third, there exist both quantum [11–13] and semi-classical [7,8] models of HHG that, although not complete as yet, can be used to carefully compare theory and experiment. Finally, as a unique type of ultrafast, coherent, short-wavelength, compact light source, HHG is a powerful tool for time resolved studies of dynamics at surfaces [14] or in chemical reactions, for X-ray imaging, and for

* Corresponding author. Fax: +1-303-492-5235.
*E-mail address:* bartels@jila.colorado.edu (R. Bartels).
[1] Permanent address: Department of Physics, Sofia University, Sofia, Bulgaria.

0301-0104/01/$ - see front matter 
PII: S0301-0104(01)00213-0

generating attosecond-duration light pulses [11, 15]. By improving the characteristics of HHG using coherent control techniques, many potential applications are enabled and made more straightforward.

The simple semi-classical theory of HHG [7,8] considers an atom immersed in an intense, ultrashort laser pulse, where the laser pulse can be treated as a time-varying electric field. At laser intensities of approximately $10^{14}$ W cm$^{-2}$, the optical field is so strong that the Coulomb barrier binding the outermost electron to the atom becomes depressed. Electrons can then tunnel through the barrier, leading to field ionization of the atom. This process occurs twice per optical cycle, during that portion of the pulse for which the laser field is sufficiently strong. Once ionized, the electrons are rapidly accelerated away from the atom by the oscillating laser field, and their trajectory is reversed when the laser field reverses. Depending on when during the optical cycle the initial tunneling event occurs, some fraction of the ionized electrons can recollide with the parent ion and recombine with it. In this recombination process, the electron kinetic energy, as well as the ionization potential energy, is released as a high-energy photon. The X-ray emission bursts occur every half-cycle ($\sim$1.2 fs) of the laser field for which the laser intensity is sufficient to ionize the atom. However, a particular harmonic (i.e. photon energy) may be emitted only during a limited number of half-cycles depending on the kinetic energy required to drive a particular harmonic. In the frequency domain, this periodic emission results in a comb of discrete harmonics of the fundamental laser, separated by twice the laser frequency. The exact nature of the emitted X-rays depends in detail on the exact waveform of the driving laser field, because this determines the phase accumulated by the electron as it oscillates in the laser field. In this paper we discuss coherent control techniques where, by precisely adjusting the exact shape (waveform) of an intense ultrashort laser pulse on a *sub-cycle* basis, we can manipulate the spectral properties of the high-harmonic emission to selectively enhance particular harmonic orders, and to generate near-transform-limited X-ray pulses for the first time [6].

Although the simple semi-classical picture of HHG described above is well established and yields very useful predictions of the general characteristics of high-harmonic radiation, a more complete description requires the use of a quantum or more rigorous semi-classical model of the evolution of the electron wave function [16]. In a quantum picture, the wave function of the atom in the intense laser field evolves in such a way that as the laser field becomes sufficiently strong, small parts of the bound-state electron wave function escape the vicinity of the nucleus and are spread over many Bohr radii ($\approx$100). This "free" portion of the electron wave function can recollide with the atomic core, and reflections from the core then lead to very rapid modulations of the electronic wave function, both in space and in time. The X-ray emission results from the resulting rapid fluctuations in the overall dipole moment of the atom: in the quasi-classical approximation, the phase of the induced dipole is determined by the value of the action at its saddle points. This corresponds to the contribution of the electron trajectories relevant to this particular emission. In the case of a linearly polarized strong field, we use the following approximate expression for the dipole moment:

$$d(\tau) = i\int_0^{\tau} d\tau_b \left[\frac{\pi}{\varepsilon + i(\tau - \tau_b)}\right]^{1.5} E(\tau_b) \times \exp\left[-iS(p_s, \tau, \tau_b) - \gamma(\tau_b)\right] \quad (1)$$

where $\varepsilon$ is a positive regularization constant, and we neglect the bare atomic dipole moments (atomic units are used here). In Eq. (1), we assume that the electron is ionized at a time $\tau_b$ by the electric field $E(t)$, and that it returns to the parent ion at a time $\tau$ after "free" motion in response to the laser field. Also, in Eq. (1) $\gamma(\tau_b) = \int_0^{\tau_b} w(t)\,dt$, where $w(t)$ is the Ammosov–Delone–Krainov [17] tunneling ionization rate, and $p_s(\tau, \tau_b) = -1/(\tau - \tau_b)\int_{\tau_b}^{\tau} A(t')\,dt'$ is the stationary momentum, for which the quasi-classical action $S(p_s, \tau, \tau_b) = \int_{\tau_b}^{\tau} dt\{1/2[p_s + A(t)]^2 + I_p\}$ has saddle points that correspond to the most relevant electron trajectories. Here $A(t)$ is the vector potential, $I_p$ is the ionization potential.

In the quantum picture, it is clear that the phase of the dipole moment of the atom, and therefore

the phase of the electric field of the emitted X-rays, depends on the accumulated phase of the electronic wave function that travels away from the core and then returns. In a simple semi-classical picture, the phase advance of the electron during the half-cycle trajectory can be estimated from the deBroglie wavelength $\lambda = \frac{h}{mv}$ to correspond to several "cycles" of the electron wave function. With this in mind, the potential for using precisely shaped driving laser pulses for "coherent control" of this system becomes more clear. Modest changes in the exact position of the creasts of the driving pulse as a function of time – that occur on a sub-optical cycle or attosecond time scale – can result in a substantial shift in phase of the X-ray burst that results from a single half-cycle of the laser field.

In the simple case where HHG is driven by an unchirped, transform-limited, laser pulse, the HHG light generated on the leading edge of the pulse, where the driving pulse intensity is rising rapidly, will be emitted with an intrinsic negative chirp. This is because the electrons released on each subsequent half-cycle traverse an increasingly longer path away from the atom, resulting in a larger phase shift of the electron wave function at the time of recollision. This results in a spectral broadening of the peaks in the HHG emission spectrum [9,10]. On the other hand, imposing a positive chirp on the driving laser pulse can counteract this intrinsic negative phase, restoring a series of well-defined harmonic emission peaks in the spectrum. In this past work, where a simple linear chirp is applied to the excitation pulse, all harmonic orders were observed to behave similarly in terms of spectral widths, and the overall X-ray flux does not increase [10].

Although past work which studied HHG excited by simple linearly chirped pulses has proven very useful in understanding the fundamental processes involved, theoretical models of HHG predict that the intrinsic chirp resulting from the electron trajectory is not in fact linear. By altering the shape of the driving laser pulse in a more sophisticated manner using a pulse shaper [2,18,19], one can expect to be able to manipulate the spectral characteristics of the XUV emission more precisely. Moreover, by adaptive feedback control of the pulse shape using an evolutionary algorithm [2,20–22], we demonstrate experimentally that we cannot only control the spectral characteristics of high-order harmonic generation, but also can very substantially enhance the overall brightness of the HHG emission in a selective fashion. Although the first finding could be expected based on past work, the second finding, that the overall efficiency of conversion of laser light to XUV light could be increased and selectively optimized, is not obvious.

The use of shaped optical pulses for controlling quantum systems was first suggested by Rabitz et al. [20–22], who demonstrated through computational simulations that trial-and-error learning algorithms can in principle be applied to optimally control quantum systems. A number of experiments have recently demonstrated the use of shaped pulses for control of quantum systems. Bardeen et al. [23] demonstrated that a learning algorithm can determine that a pulse with positive chirp is optimally effective in avoiding saturation of a molecular transition. Silberberg et al. [24] showed that introducing a phase jump into a short pulse could be used to modulate two-photon absorption, as a result of interference effects. Gerber et al. [25] demonstrated that molecular dissociation could be controlled through the use of pulses with a complex shape determined through a learning algorithm. Bucksbaum et al. [26,27] demonstrated the use of iterative algorithms to "sculpt" Rydberg atom wave functions into the desired configuration, and also to control Stokes scattering in molecular systems. These experiments represent systems at the two extremes of complexity. In the case of one- and two-photon absorption or molecular excitation, the physical reasons behind the optimum solutions are straightforward to understand. In the case of vibrational excitation or dissociation of polyatomic molecules, the pulse shapes obtained through optimization are complex and extremely difficult to interpret.

In contrast, the case of HHG represents a quantum process that is highly nonlinear, but that nevertheless has proven to be both accessible to experiment and theoretically tractable. The optimal laser pulse for coherent X-ray generation can be explained as a new type of "intra-atomic" phase

matching [13], that enhances the constructive interference of the X-ray emission from different electron trajectories driven by adjacent optical cycles for a particular wavelength (i.e. harmonic order). This intra-atomic phase matching allows us to selectively increase the brightness of a single harmonic order by over an order of magnitude, essentially channeling the nonlinear response of the atom into a particular order of nonlinearity. Furthermore, the arbitrary control over the shape of the driving pulse allows us to spectrally narrow a given harmonic order very effectively, resulting in a bandwidth of the harmonic peak that is likely to be at or near the time-bandwidth limit for such a short X-ray pulse. Finally, optimization of a single harmonic without suppressing adjacent harmonics can increase the brightness of some harmonic orders by factors of 30.

## 2. Experiment

The process of HHG is best implemented using very short-duration ($\ll$100 fs) light pulses. This allows a relatively high intensity to be incident on a neutral atom prior to ionization, resulting in more-efficient generation of higher-energy harmonic photons [28–30]. For our work, we used a short-pulse-optimized Ti:sapphire amplifier system into which a closed-loop pulse shaping apparatus was incorporated [2]. By careful design of these amplifier systems, pulses as short as 15 fs (approximately six optical cycles) FWHM can be generated at high repetition rates and high pulse energies (up to 7 kHz with pulse energies $> 1$ mJ). In such laser systems, low energy pulses of duration $\sim$10 fs are generated by a broad-bandwidth Ti:sapphire oscillator, stretched in time to lower their peak intensity, and then amplified in one to two amplifier crystals prior to recompression. This type of laser system is ideal for inclusion of a simple, phase-only, pulse shaper into the beam before amplification, since phase modulations introduced by the shaper will remain present without distortion in the high-energy, amplified laser pulse.

We used a new type of phase-only pulse shaper for this work, incorporating a micromachined deformable mirror [2,19]. This simple shaper works by separating the color components of the ultrashort light pulse (which span $\sim$80 nm bandwidth centered on 800 nm) using a grating, then reflecting them from the deformable mirror. Subsequently, the color components are reassembled to form a collimated, temporally shaped, beam. Altering the exact shape of the mirror can then control the relative arrival time of each color component in the pulse. Thus, the pulse shaper manipulates the phase of the pulse in the spectral domain, reshaping the pulse shape and phase in the time domain, while conserving pulse energy. The mirror itself is a smooth silicon-nitride surface incorporating 19 actuators that deform the mirror – thus it is possible to precisely control the pulse shape, without introducing ''artifacts'' due to discrete pixellation. Although this type of pulse shaper is limited in that it is a ''phase-only'' shaper and cannot alter the spectrum of the driving pulse, this has not been proven to be a significant limitation in controlling a highly nonlinear process such as HHG: color components that are not wanted can always be moved to early or late times within the pulse where no HHG is taking place. Furthermore, by not altering the spectrum of the pulse, we avoid possible pulse distortions due to nonlinear self-phase modulation in the amplifier. The exact shape of the pulse, including the amplitude and phase of the electromagnetic field, can be measured using the second-harmonic generation frequency resolved optical gating (SHG FROG) technique [31].

The difficulty of calibrating the pulse shaper to generate a predetermined pulse shape, as well as the uncertain accuracy of theoretical models that might predict an optimum pulse shape, make a ''one-step'' optimization of the HHG process both impractical and undesirable. Instead, we implemented a trial-and-error learning algorithm to train the laser system to optimize the high-harmonic emission, thus controlling the response of the atomic wave function to obtain an optimal outcome. We used an evolutionary algorithm, that starts with a collection of population ''members'', each of which corresponds to a particular set of voltages applied to the 19 mirror actuators. The ''fitness'' of the corresponding pulse shape is then measured experimentally. The fitness is simply a

quantitative measure of the desirability of a population member; for example the brightness of a particular high-harmonic peak. The best solutions (largest fitness values) are selected as parents, which determine future populations (generation) of the algorithm. Several copies of each parent form the set of children. The children are mutated with a Gaussian noise function to perturb the solutions. The parents and mutated children are combined to form the population of the next generation. The process is then repeated until the fitness changes by an insignificant amount between generations; at this point, the process is said to have converged. This typically occurs in 50–100 iterations, with about 100 population members tested for each iteration.

This scheme requires a large number of repeated trials, which is possible in a reasonable time because of the high photon flux generated through phase-matched HHG [32]. In phase-matched frequency conversion, an environment is created where both the fundamental and the harmonic radiation travel through an extended medium at the same phase velocity. This allows the nonlinear signal of all atoms within this region to add coherently and constructively, enhancing the output signal. *Phase matching is characterized by a reduction of destructive interference in order to increase total harmonic signal levels*. In conventional nonlinear optics at visible wavelengths, phase matching is typically accomplished using a birefringent crystal oriented such that the pump beam (in one polarization) and the signal (in another) travel at the same speed. In the case of HHG, the XUV light propagates in a low-pressure, isotropic gas, precluding the use of birefringence effects. Instead, we propagate the light in a waveguide structure (simply a hollow capillary tube), and use the frequency-dependent phase velocity of the waveguide, in combination with the gas dispersion, to achieve phase matching. In the case of phase-matched HHG, the total conversion efficiency is still limited by effects such as the strong absorption of the HHG radiation in the gas, and the effects of ionized electrons on phase matching. Nevertheless this technique allows us to achieve conversion efficiencies of $\sim 10^{-5}$ to photons energies of $\sim 50$ eV, while also using a kilohertz repetition-rate, millijoule pulse-energy laser system. The resulting flux is sufficient to obtain a high signal-to-noise high-harmonic spectrum in a single shot using a flat-field X-ray spectrometer. In practice, our apparatus can try $\sim 100$ different pulse shapes per second. Equally important, since the output signal we observe results from an in-phase coherent addition of individual atomic responses, many effects and distortions of the pulse spectrum that might result as a result of propagation are minimized – essentially, phase matching allows us to approach the "single atom" response to the driving laser. Experimentally, we observed that our optimization process works best in the parameter range corresponding to phase matching; this finding is corroborated by the fact that our "single atom" theoretical models, as discussed below, are consistent with experimental findings.

To demonstrate that the evolutionary algorithm selects a pulse shape unique to optimizing the HHG, we preceded each HHG optimization run with a pulse-duration optimization. This allows us to start with a time-bandwidth-limited pulse, and see how the HHG optimized pulse differs from it. The time-bandwidth-limited pulse is obtained by using the evolutionary algorithm with a feedback signal derived from second-harmonic generation of the pulse [2,19,33]. A fraction of the laser output is sent into a second-harmonic crystal. The conversion efficiency of the SHG increases with the peak intensity of the fundamental pulse; thus the most intense pulse, which occurs when all component frequencies of the pulse have the same relative arrival time, produces the largest fitness value and corresponds to the Fourier transform-limited pulse. This computer optimization converges after about 100 generations of about 100 trials each (10,000 total "experiments"). This optimization takes $\sim 10$ min of real time, and converges very well to a transform-limited pulse, as was verified by making FROG measurements on the pulse.

Subsequent to this optimization, the HHG optimization is performed. The set-up is shown in Fig. 1. The X-ray output from a hollow core fiber is passed through a 100 nm aluminum filter to eliminate the fundamental IR beam, while passing photon energies up to 72 eV. An imaging X-ray

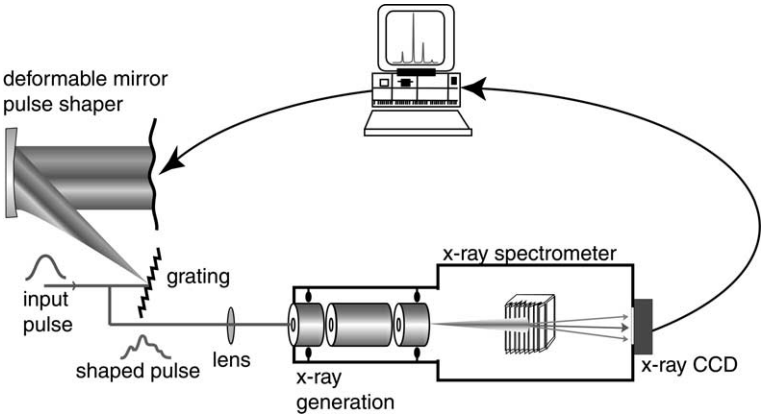


Fig. 1. Experimental set-up for optimization of HHG.

spectrometer (Hettrick SXR-1.75) was used to image the spectrum onto an X-ray CCD camera (Andor Technologies). A computer reads in the HHG spectrum and evaluates the fitness criterion. The fitness functions used to evaluate the harmonic spectrum will differ depending on the goals of the optimization process. A particular harmonic is designated as the spectral flux ($s_j$) integrated over a 0.5 eV bandwidth about that harmonic (corresponding to the resolution limit of our spectrometer/CCD system). Table 1 lists a number of fitness functions we used for various optimization goals. The simplest fitness criterion to use is simply to observe the peak intensity of a single-harmonic order (Table 1(a)). Alternatively, it is possible to select for enhancement primarily of only one harmonic order (Table 1(c)). Fig. 2 shows the result of such an optimization at 50 Torr of Argon gas pressure in a 175 μm diameter fused silica capillary 29 mm long. This pressure is optimum for phase matching in this geometry. We see that the intensity of the 27th harmonic can be increased by a factor of eight over that which was obtained using a transform-limited pulse. Furthermore, the brightness of other harmonic orders does not increase as much, and the spectral bandwidth of the harmonic order decreases. This is very desirable for application experiments such as time-resolved photoelectron spectroscopy that require monochromatic emission.

The result discussed above is remarkable in that we have shown that although second-harmonic emission is optimized using the highest peak-power, transform-limited pulse, *high*-harmonic emission is optimized with a nontransform-limited pulse. This is a manifestation of the fact that HHG is fundamentally a nonperturbative process – slight changes in pulse shape can "channel" exci-

Table 1
Various fitness functions used by the learning algorithm

| | Goal | Form | Notation |
|---|---|---|---|
| (a) | Increase brightness | $f := (s_{j,k}: s_{j,k} \geqslant s_{j,i}\ \forall i)$ | $M_j$ |
| (b) | Increase energy | $f := \Sigma s_{j,i}$ | $E_j$ |
| (c) | Select single harmonic and suppress neighbor energies | $f := E_j - \frac{1}{2}(E_{j-2} + E_{j+2})$ | |
| (d) | Select single harmonic and suppress neighbor brightness | $f := M_j - \frac{1}{2}(M_{j-2} + M_{j+2})$ | |

$s_j$ refers to the $j$th harmonic spectrum. (a) Finds the maximum value of a given harmonic order, (b) finds the energy of a given harmonic order with summation over $i$, (c) selects a single harmonic order with an energy criterion, and (d) selects a single harmonic order with a brightness criterion.

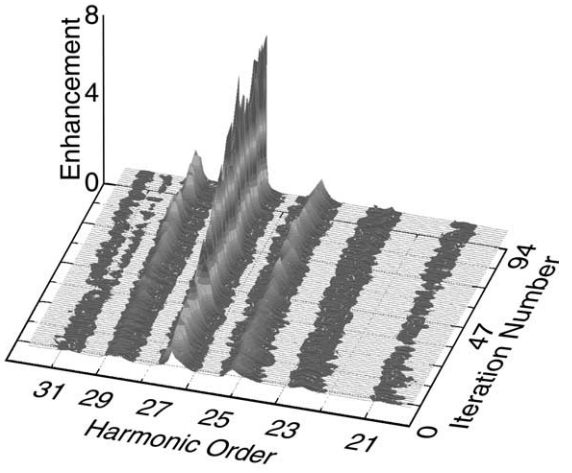


Fig. 2. Optimization of a single (27th) harmonic in argon while suppressing adjacent harmonics.

tation from one harmonic order to another. The optimized pulse shape is actually only slightly different from the transform limit – 21 fs as opposed to the 18 fs transform limit. Fig. 3 shows the laser pulse shapes corresponding to the transform-limited and final (iteration number 94) HHG spectra shown in Fig. 2. The initial pulse is quite smooth and nearly transform limited while the optimized pulse is slightly broader with some additional nonlinear chirp on the leading edge of the pulse. Thus, a very slight change in the pulse used to drive the HHG process can result in a substantial and beneficial change in the output energy, brightness, and spectrum of the HHG radiation.

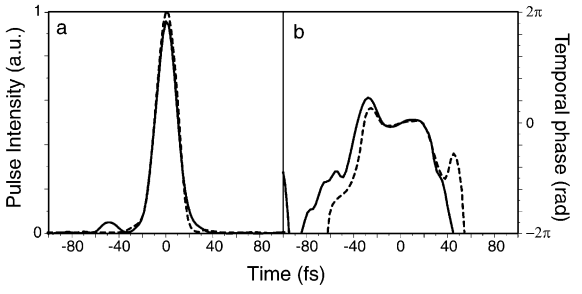


Fig. 3. Amplitude and phase of the laser pulses corresponding to Fig. 2: (a) initial transform-limited pulse (- - -) and optimized pulse shape (—); (b) initial (- - -) and optimized temporal phase (—).

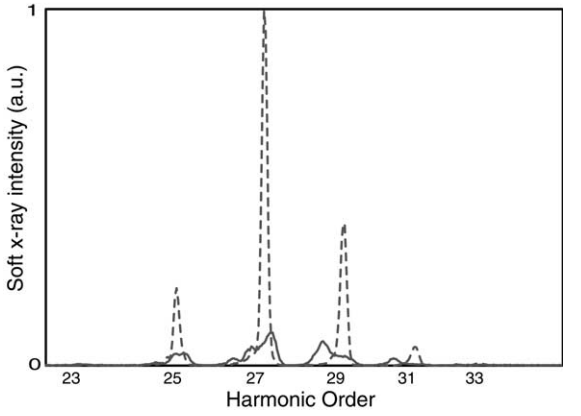


Fig. 4. Optimization of a single harmonic in argon with a spectral window at longer wavelengths than in Fig. 2 and without suppressing adjacent harmonics. The harmonic peak is enhanced by over an order of magnitude. Harmonics before and after optimization are shown by solid and dashed respectively.

Other fitness criteria select different optimal outcomes. Fig. 4 shows the results of an optimization run in which the brightness of the 27th harmonic is used as the fitness criterion. In this solution, the brightness of the harmonic is increased by more than an order of magnitude. The spectral resolution of the measured spectral width shown in Fig. 4 is instrument limited at 0.24 eV FWHM; before optimization the bandwidth of this harmonic peak was $>1$ eV. This optimized bandwidth corresponds to a transform-limited pulse duration of $\sim$5 fs. Under similar conditions, simulations also predict an X-ray pulse duration of $\approx$5 fs. Thus, the optimization process can likely generate near-transform-limited X-ray pulses for certain fitness criteria. Fig. 5 shows the highest enhancements we have observed to date. Here, the 21st harmonic is observed to increase by a factor of 33 when excited by an optimized pulse compared with a transform-limited excitation pulse.

Although the data of Figs. 4 and 5 show the highest enhancement observed in our experiments to date, all harmonics optimized in any noble gas exhibit some enhancement of the X-ray signal after optimization. As an example, Fig. 6 shows the results of a series of experiments in which successive individual harmonic orders (17–23) were

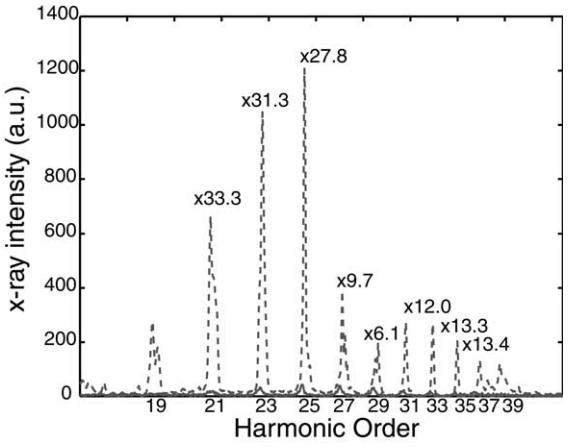


Fig. 5. Highest enhancements observed to date. The 21st harmonic is observed to increase by a factor of 33 when excited by an optimized pulse compared with a transform-limited excitation pulse. Harmonics before and after optimization are shown by solid and dashed respectively.

optimized in Krypton at a pressure of 4 Torr. The fitness function used for these harmonics is that of Table 1(d). Each harmonic order optimization was successful to varying degrees with brightness increases from 1.7 to 6 and increases of the energy in the optimized harmonic order from 5% to 220%. To distinguish between the optimized pulses corresponding to the series of harmonics shown in Fig. 6, a Wigner distribution (a type of time-frequency representation of the pulse) can be used. We observe that the optimal pulse shape results from spectral phase changes in different spectral regions of the pulse for each optimization of Fig. 6.

As the energy of the driving laser pulse increases, the X-ray emission becomes stronger and then eventually saturates, as shown in Fig. 7(a). This saturation is accompanied by a reduction in the rms fluctuations of the X-ray output, as shown in Fig. 7(b). Also plotted on this figure is the peak enhancement factor of a single-harmonic order as a function of driving pulse energy. At low pulse energy, the enhancement factor is very weak. However as the pulse energy increases, the enhancement factor also increases. Once the HHG process saturates, the driving laser pulse can be stretched to a longer duration while still having sufficient intensity to create the necessary harmonic orders, providing freedom to change the pulse shape or waveform in order to optimize the harmonics. By contrast, prior to saturation, the necessary pulse shape changes to the driving laser pulse often reduce the peak intensity of the pulse sufficiently such that the particular harmonic order can no longer be generated.

## 3. Theory

Very recently, we have developed a successful theoretical model of this HHG optimization process that explains the physical basis of the optimization [13]. Using this model, we can show that a new type of phase matching is possible when an atom is driven by an optimal optical waveform. This model is a highly optimized version of the Lewenstein model [16] that calculates HHG spectra in a semi-classical approximation. We apply a learning algorithm to the model, which runs at speeds comparable to the experiment, and which applies the same fitness functions to the HHG emissions as in the experimental optimization. The model predicts an optimized pulse shape and emission spectrum that is very close to the experimental results – in the case of selective optimization of a single peak, for example, an enhancement of $\sim 8\times$ is predicted, using an optimized laser pulse shape slightly longer than the transform limit. Fig. 8 shows the experimental and calculated optimized laser pulse shapes, together with the corresponding phase. There is excellent agreement, with both pulses exhibiting a nonlinear "chirp" on the leading edge. The trailing edge of the pulse in either case is random – as expected since HHG occurs on the leading edge of the pulse. Therefore our fitness functions do not select any particular shape for the trailing edge of the pulse.

Our model is a novel theoretical approach to HHG that couples a fully quantum model of the electron response with a semi-classical electron trajectory picture. In the quasi-classical model, the X-ray emission results from rescattering of an electron, ionized in a strong laser field, with its parent ion. In our approach, each harmonic order appears as a result of a constructive or destructive

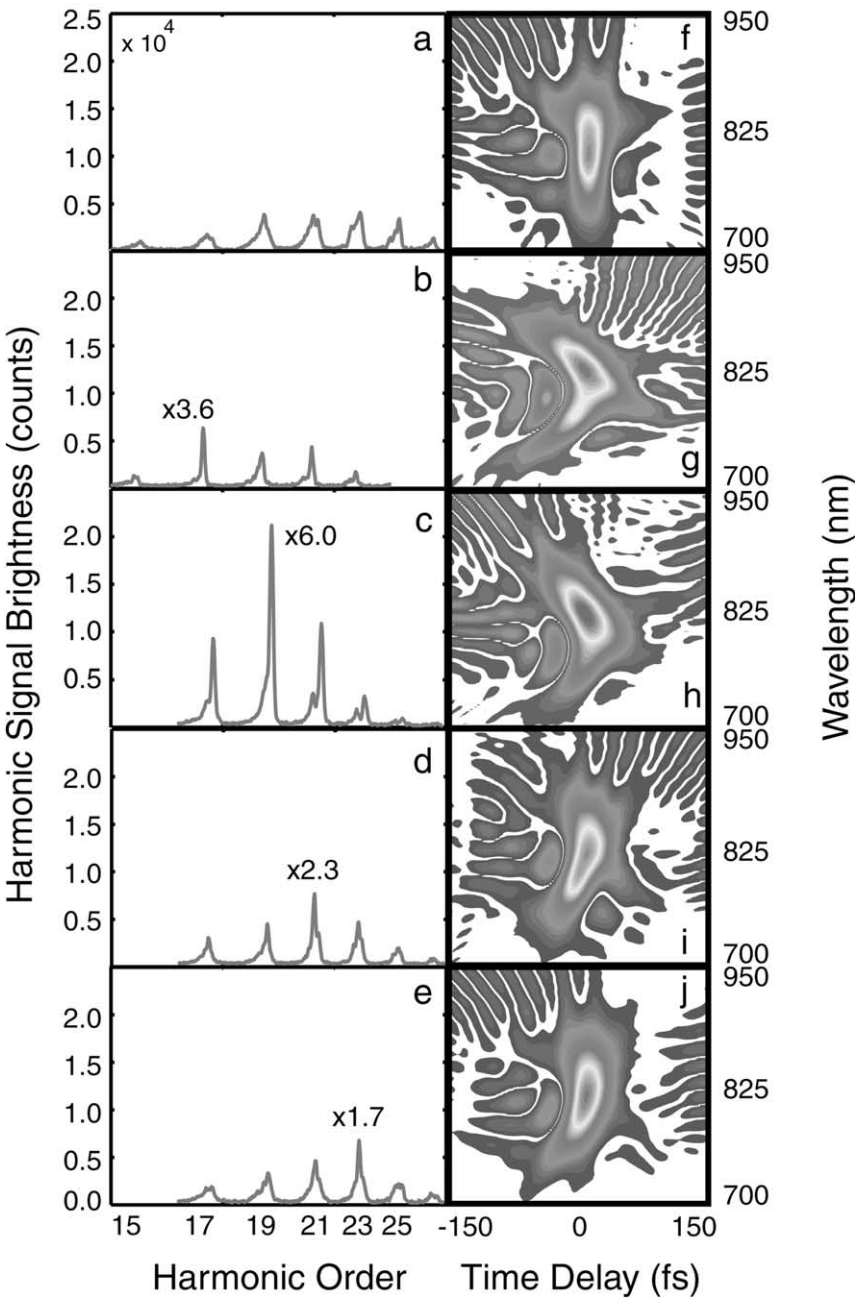


Fig. 6. Sequence of optimizations performed in Kr for adjacent harmonics (17–23). (a) Measured harmonic spectra for the transform limit and after optimization with the fitness criterion in Table 1(d) for (b) the 17th, (c) 19th, (d) 21st, and (e) 23rd order harmonics. The Wigner distributions for the measured transform-limited and optimal pulse shapes are shown in panels (f)–(j) next to their corresponding spectra.

interference of the contributions of a number of rescattered electron trajectories. Since the amplitude and the phase of the contribution of a given electron trajectory to the dipole moment is directly

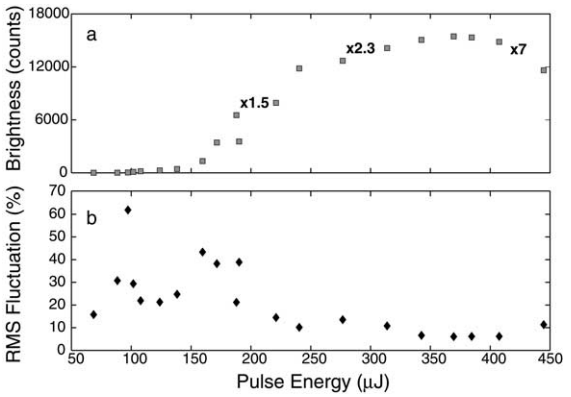


Fig. 7. (a) X-ray emission as a function of driving laser energy for an optimal laser pulse shape along with brightness enhancement factors of the 29th harmonic in argon as a function of driving pulse energy. (b) RMS fluctuations of the X-ray output, as a function of driving laser intensity.

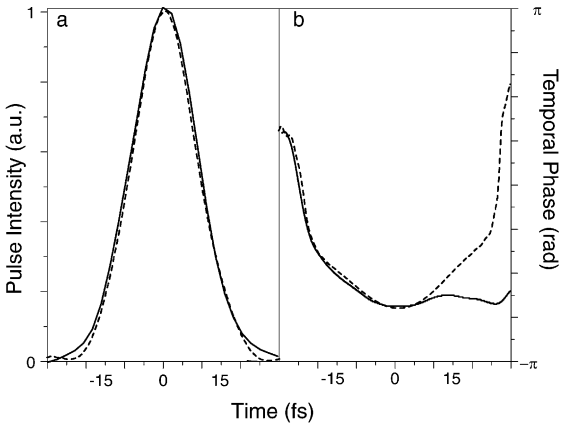


Fig. 8. Experimental and calculated optimized laser pulse shapes, together with the corresponding phase. The experimental phase trace is the difference between the measured optimized and initial temporal phase in Fig. 3(b) scaled by a factor of four in amplitude.

related to the amplitude and the phase of the laser field at the time of ionization, it is intuitively clear that by shaping the waveform of the laser pulse, one may control the interference effects in the X-ray emission that comes from these different electron trajectories. In this way, a significant redirection of energy between the different harmonics within the harmonic comb is possible. Such improvements are not possible by simply changing the linear chirp of the driving laser pulse, as has been demonstrated previously [10].

Fig. 9 illustrates the essence of the optimization process. In Fig. 9(a), the dotted line shows the time dependence of the phase of the 25th harmonic when generated by a transform limited pulse. This dependence is close to parabolic, which reflects the effect of the laser-induced intrinsic phase of the atomic dipole. In contrast, the phase dependence for the optimized laser pulse (solid line) is almost flat, with a phase error corresponding to a time delay of less than 25 as – which is considerably smaller than the period of the 25th harmonic (106 as). This effect can be interpreted as a phase matching that takes place between the atom and the laser pulse, ensuring that the phases of the contributions from different electron trajectories are locked within a narrow time interval. This leads to a strong positive interference effect in the frequency domain, optimizing the temporal coherence of the harmonic field. Fig. 9(b) shows the temporal phase of the trajectories that contribute to the 23rd and 29th harmonic orders for the identical laser pulse shape which optimizes the 25th harmonic (Fig. 8). It can be seen that the optimal pulse shape for the 25th harmonic "overcompensates" the phase for lower-order harmonics and "under-compensates" the phase for higher order harmonics.

This model clearly illustrates the physics behind the shaped-pulse optimization and demonstrates that the optimization results from a single-atom effect. The total X-ray signal is the result of coherent interference of the emissions resulting from a number of electron trajectories that emit the correct photon energy on recollision, as illustrated schematically in Fig. 10. From Fig. 8, it is clear that the phase of the optimized laser pulse corresponds to a high-order nonlinear chirp, which determines the "correct" release time and phase of the various half-cycles of the electromagnetic field to ensure that the continuum generated during each half-cycle of the pulse reinforces constructively or destructively with parts of the continuum generated by adjacent half-cycles. From a quantum point of view, the optimized laser field creates an extended electron wavepacket with appropriate spatial modulation along the direction of polar-

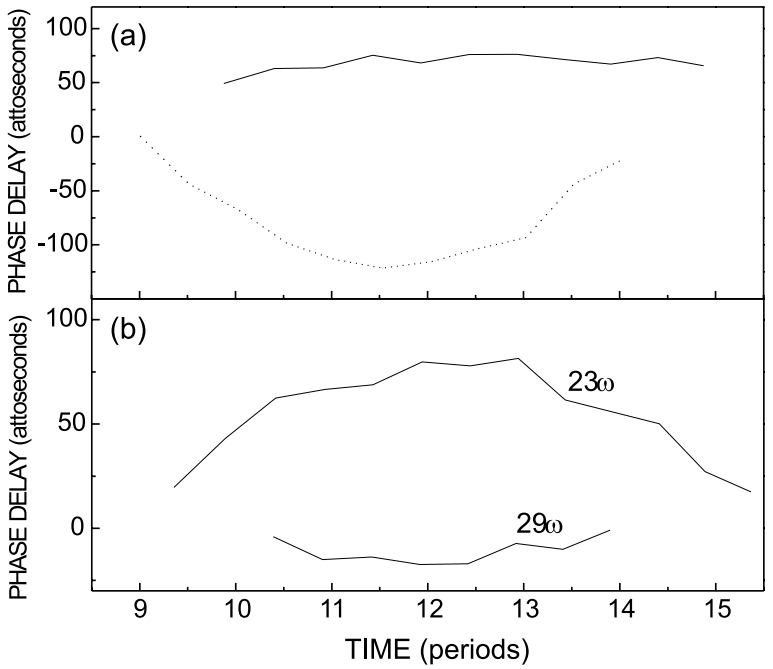


Fig. 9. (a) Phase distribution of the most relevant trajectories before (- - -) and after (—) optimization. (b) Phase distribution of neighboring harmonic orders after optimization.

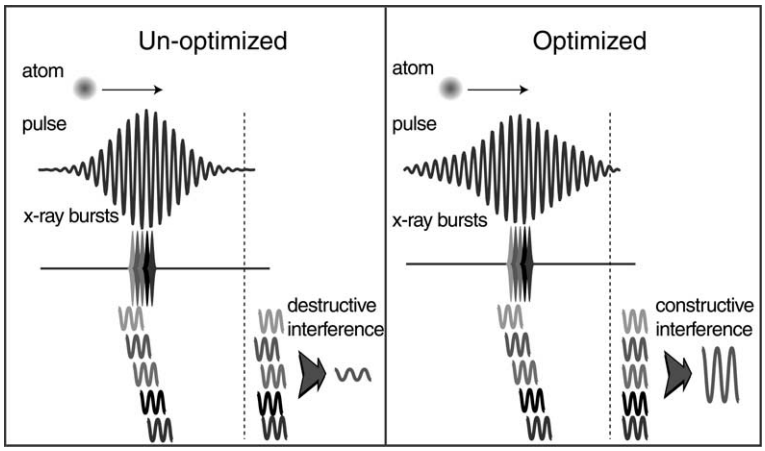


Fig. 10. Schematic representation of intra-atomic phase matching.

ization, which on recollision results in stronger generation of the optimized harmonic. In the X-ray cell, the laser pulses are propagating through atoms that are essentially stationary with respect to the fundamental pulse. Alternatively, we can view this as atoms traveling through stationary laser pulses. In this picture, each time the atom passes through a half-cycle of the laser pulse, an X-ray burst is generated. If we filter out the target harmonic, we can view this as a series of short,

narrow-bandwidth X-ray bursts. In general, for a transform-limited pulse the phases of these individual trajectories do not add wholly constructively. On the other hand, the optimized pulse shape clearly shows that the classical trajectories resulting in that harmonic energy are now precisely "in-phase". The pulse-shaping results in timing adjustments *within the laser pulse* that correspond to coherent control of the electron wave function evolution on a sub-optical cycle 25 as time scale.

Manipulating the phase of the X-ray bursts such that they add together constructively generates a larger X-ray flux due to *a reduction of destructive interference pathways*. This is exactly analogous to traditional phase matching. The observed increase in total X-ray flux as a result of rephasing of harmonic emission therefore represents a new type of intra-atomic phase matching during the laser–atom interaction, that occurs on a sub-optical cycle or attosecond time scale.

## 4. Summary

In summary, this work demonstrates adaptive or "learning" control of a very high-order nonlinear process in the strong-field regime for the first time. We demonstrate significantly increased enhancement and selectivity of individual harmonic orders, as well as the generation of near-transform-limited X-ray pulses. Both theory and experiment confirm that we achieve optimization and control of the HHG process by adjusting the relative timing of the crests of the optical wave on a sub-cycle or attosecond time scale. This adjustment changes the recollision time of an electron with an ion with a precision of 25 as. Furthermore, we have shown that this optimization process has uncovered a new type of intra-atomic phase matching. For an optimized laser pulse shape, strong constructive interference can be obtained in the frequency domain between different electron trajectories generated from different half-cycles of a laser pulse, thereby optimizing a particular high-harmonic order. Microscopically, the optimized laser pulse shaped is mapped onto oscillations in the wave function of the ionizing electron, thus generating an optimized atomic dipole moment for X-ray generation. Our results have immediate utility for the probing of dynamics of chemical and material systems, because it provides a way to select a harmonic without temporally broadening it. The result is a bright, quasi-monochromatic, transform-limited, and highly spatially coherent soft X-ray light source for use in techniques such as photoelectron spectroscopy and spectromicroscopy, time-resolved X-ray studies of material and chemical systems, and time-resolved holographic imaging. Finally, HHG should also provide a fruitful testbed for further work in quantum control concepts, because theoretical models are available to aid in understanding the outcome of optimization. For example, the speed and robustness of different algorithms can be evaluated, to learn more about multi-parameter optimization. Finally, we note that the application of an evolutionary learning algorithm resulted in our obtaining a deeper understanding of the dynamics of this quantum system; i.e. "learning" algorithms really do resulting in *learning*.

## Acknowledgements

The authors gratefully acknowledge support from the National Science Foundation and from the Department of Energy. R. Bartels acknowledges support from a National Defense Science and Engineering Graduate Fellowship.

## References

[1] S. Backus, C. Durfee, M.M. Murnane, H.C. Kapteyn, Rev. Sci. Instrum. 69 (1998) 1207.
[2] E. Zeek, R. Bartels, M.M. Murnane, H.C. Kapteyn, S. Backus, G. Vdovin, Opt. Lett. 25 (2000) 587.
[3] A. McPherson, G. Gibson, H. Jara, U. Johann, T.S. Luk, I.A. McIntyre, K. Boyer, C.K. Rhodes, J. Opt. Soc. Am. B 4 (1987) 595.
[4] A. L'Huillier, K.J. Schafer, K.C. Kulander, Phys. Rev. Lett. 66 (1991) 2200.
[5] J.J. Macklin, J.D. Kmetec, C.L. Gordon III, Phys. Rev. Lett. 70 (1993) 766.
[6] R. Bartels, S. Backus, E. Zeek, L. Misoguti, G. Vdovin, I.P. Christov, M.M. Murnane, H.C. Kapteyn, Nature 406 (2000) 164.

[7] K.C. Kulander, K.J. Schafer, J.L. Krause, Super-intense laser-atom physics, in: B. Piraux, A. L'Huillier, K. Rzazewski (Eds.), NATO Advanced Science Institutes Series, vol. 316, Plenum Press, New York, 1993, p. 95.
[8] M. Lewenstein, P. Balcou, M.Y. Ivanov, P.B. Corkum, Phys. Rev. A 49 (1993) 2117.
[9] P. Salieres, P. Antoine, A. de Bohan, M. Lewenstein, Phys. Rev. Lett. 81 (1998) 5544.
[10] Z. Chang, A. Rundquist, H. Wang, I. Christov, H.C. Kapteyn, M.M. Murnane, Phys. Rev. A 58 (1998) R30.
[11] I.P. Christov, M.M. Murnane, H.C. Kapteyn, Phys. Rev. Lett. 78 (1997) 1251.
[12] I.P. Christov, M.M. Murnane, H.C. Kapteyn, Phys. Rev. A 57 (1998) R2285.
[13] I.P. Christov, R. Bartels, S. Backus, H.C. Kapteyn, M.M. Murnane, Phys. Rev. Lett., submitted for publication.
[14] R. Haight, Surf. Sci. Rep. 21 (1995) 275.
[15] P.B. Corkum, N.H. Burnett, M.Y. Ivanov, Opt. Lett. 19 (1994) 1870.
[16] M. Lewenstein, P. Balcou, M.Y. Ivanov, A. Lhuillier, P.B. Corkum, Phys. Rev. A 49 (1994) 2117.
[17] M.V. Ammosov, N.B. Delone, V.P. Krainov, Soviet Phys. JETP 64 (1986) 1191.
[18] A.M. Weiner, J.P. Heritage, E.M. Kirschner, J. Opt. Soc. Am. B – Opt. Phys. 5 (1988) 1563.
[19] E. Zeek, K. Maginnis, S. Backus, U. Russek, M. Murnane, G. Mourou, H. Kapteyn, G. Vdovin, Opt. Lett. 24 (1999) 493.
[20] R. Judson, H. Rabitz, Phys. Rev. Lett. 68 (1992) 1500.
[21] H. Rabitz, Adv. Chem. Phys. 101 (1997) 315.
[22] H. Rabitz, R. de Vivie-Riedle, M. Motzkus, K. Kompa, Science 288 (2000) 824.
[23] C.J. Bardeen, V.V. Yakovlev, K.R. Wilson, S.D. Carpenter, P.M. Weber, W.S. Warren, Chem. Phys. Lett. 280 (1997) 151.
[24] D. Meshulach, Y. Silberberg, Nature 396 (1998) 239.
[25] A. Assion, T. Baumert, M. Bergt, T. Brixner, B. Kiefer, V. Seyfried, M. Strehle, G. Gerber, Science 282 (1998) 919.
[26] T.C. Weinacht, J.L. White, P.H. Bucksbaum, J. Phys. Chem. a 103 (1999) 10166.
[27] T.C. Weinacht, J. Ahn, P.H. Bucksbaum, Nature 397 (1999) 233.
[28] J. Zhou, J. Peatross, M.M. Murnane, H.C. Kapteyn, I.P. Christov, Phys. Rev. Lett. 76 (1996) 752.
[29] Z.H. Chang, A. Rundquist, H.W. Wang, M.M. Murnane, H.C. Kapteyn, Phys. Rev. Lett. 79 (1997) 2967.
[30] C. Spielmann, N.H. Burnett, S. Sartania, R. Koppitsch, M. Schnürer, C. Kan, M. Lenzner, P. Wobrauschek, F. Krausz, Science 278 (1997) 661.
[31] K.W. DeLong, R. Trebino, J. Hunter, W.E. White, J. Opt. Soc. Am. B 11 (1994) 2206.
[32] A. Rundquist, C.G. Durfee III, S. Backus, C. Herne, Z. Chang, M.M. Murnane, H.C. Kapteyn, Science 280 (1998) 1412.
[33] D. Yelin, D. Meshulach, Y. Silberberg, Opt. Lett. 222 (1997) 1793.